Letter

^{3}He($\vec{n}$, p)^{3}H parity-conserving asymmetry

M. Viviani,[1,*] S. Baeßler,[2,3] L. Barrón-Palos,[4] N. Birge,[5,6] J. D. Bowman,[3] J. Calarco,[7] V. Cianciolo,[3] C. E. Coppola,[5] C. B. Crawford,[8] G. Dodson,[9] N. Fomin,[5] I. Garishvili,[3,5] M. T. Gericke,[10] L. Girlanda,[11,12] G. L. Greene,[5,3] G. M. Hale,[6] J. Hamblen,[13] C. Hayes,[5,14] E. B. Iverson,[3] M. L. Kabir,[8,15] A. Kievsky,[1] L. E. Marcucci,[16,1] M. McCrea,[10,17] E. Plemons,[5] A. Ramírez-Morales,[4] P. E. Mueller,[3] I. Novikov,[18] S. I. Penttila,[3] E. M. Scott,[5,19] J. Watts,[13] and C. Wickersham[13]
(n3He Collaboration)
[1]*Istituto Nazionale di Fisica Nucleare, Sezione di Pisa, I-56127 Pisa, Italy*
[2]*University of Virginia, Charlottesville, Virginia 22904, USA*
[3]*Oak Ridge National Laboratory, Oak Ridge, Tennessee 37831, USA*
[4]*Instituto de Física, Universidad Nacional Autónoma de México, Apartado Postal 20-364, 01000, México*
[5]*University of Tennessee Knoxville, Knoxville, Tennessee 37996, USA*
[6]*Los Alamos National Laboratory, Los Alamos, New Mexico 87545, USA*
[7]*University of New Hampshire, Durham, New Hampshire 03824, USA*
[8]*University of Kentucky, Lexington, Kentucky 40506, USA*
[9]*Massachusetts Institute of Technology, Cambridge, Massachusetts 02139, USA*
[10]*University of Manitoba, Manitoba R3T 2N2, Canada*
[11]*Department of Mathematics and Physics, University of Salento, I-73100 Lecce, Italy*
[12]*Istituto Nazionale di Fisica Nucleare, Sezione di Lecce, I-73100 Lecce, Italy*
[13]*University of Tennessee Chattanooga, Chattanooga, Tennessee 37403, USA*
[14]*Indiana University, Bloomington, Indiana 47405, USA*
[15]*Brookhaven National Laboratory, Upton, New York 11973, USA*
[16]*Department of Physics "E. Fermi", University of Pisa, I-56127, Pisa, Italy*
[17]*University of Winnipeg, Winnipeg, Manitoba R3B 2E9, Canada*
[18]*Western Kentucky University, Bowling Green, Kentucky, 42101, USA*
[19]*Centre College, Danville, Kentucky 40422, USA*

(Received 27 May 2024; accepted 31 October 2024; published 24 December 2024)

Recently, the n^3He Collaboration reported a measurement of the parity-violating (PV) proton directional asymmetry $A_{\rm PV} = [1.55 \pm 0.97\,({\rm stat}) \pm 0.24\,({\rm sys})] \times 10^{-8}$ in the capture reaction of ^{3}He($\vec{n}$, p)^{3}H at meV incident neutron energies. The result increased the limited inventory of precisely measured and calculable PV observables in few-body systems required to further understand the structure of hadronic weak interaction. In this Letter, we report the experimental and theoretical investigation of a parity conserving (PC) asymmetry $A_{\rm PC}$ in the same reaction (the first ever measured PC observable at meV neutron energies). As a result of S- and P-wave mixing in the reaction, the $A_{\rm PC}$ is inversely proportional to the neutron wavelength λ. The experimental value is $(\lambda \times A_{\rm PC}) \equiv \beta = [-1.97 \pm 0.28\,({\rm stat}) \pm 0.12\,({\rm sys})] \times 10^{-6}$ Å. We present results for a theoretical analysis of this reaction by solving the four-body scattering problem within the hyperspherical harmonic method. We find that in the ^{3}He($\vec{n}$, p)^{3}H reaction, $A_{\rm PC}$ depends critically on the energy and width of the close 0^- resonant state of ^{4}He, resulting in a large sensitivity to the spin-orbit components of the nucleon-nucleon force and even to the three-nucleon force. The analysis of the accurately measured $A_{\rm PC}$ and $A_{\rm PV}$ using the same few-body theoretical models gives essential information needed to interpret the PV asymmetry in the ^{3}He($\vec{n}$, p)^{3}H reaction.

DOI: 10.1103/PhysRevC.110.L061001

Introduction. The study of polarization observables in nuclear reactions is an important tool, in some cases the only tool, to improve our understanding on issues ranging from fundamental symmetries to still ambiguous observations in the strong nuclear interaction. In this Letter we present results from an investigation of the reaction of ^{3}He($\vec{n}$, p)^{3}H using transverse polarized neutrons of meV energies at the Spallation Neutron Source (SNS) of the Oak Ridge National Laboratory (ORNL). In a previous paper, we reported the parity-violating (PV) asymmetry $A_{\rm PV} = [1.55 \pm 0.97\,({\rm stat}) \pm 0.24\,({\rm sys})] \times 10^{-8}$ [1]. Here, we present the experimental and theoretical investigation of a parity-conserving (PC) asymmetry in the reaction. In general, the cross section for ^{3}He($\vec{n}$, p)^{3}H can be written as

$$\frac{{\rm d}\sigma}{{\rm d}\Omega} = \left(\frac{{\rm d}\sigma}{{\rm d}\Omega}\right)_{\rm u} (1 + A_{\rm PV}\hat{s}_{\rm n} \cdot \hat{k}_{\rm p} + A_{\rm PC}(\hat{s}_{\rm n} \times \hat{k}_{\rm n}) \cdot \hat{k}_{\rm p}), \quad (1)$$

*Contact author: michele.viviani@pi.infn.it

where $(d\sigma/d\Omega)_u$ is the unpolarized cross section and $\hat{s}_n$, $\hat{k}_p$, and $\hat{k}_n$ denote unit vectors specifying the directions of the neutron polarization, the outgoing proton momentum, and the incoming neutron beam, respectively. The A_{PC} is measured by detecting emitted protons with their momenta in the plane defined by $\hat{s}_n \times \hat{k}_n$ and $\hat{k}_n$, and the A_{PV} in the plane $\hat{s}_n$ and $\hat{k}_n$. The asymmetry is deduced from detector yields with opposite neutron spin direction.

At a fundamental level, PV observables in nuclei are a consequence of the hadronic weak interaction (HWI) between quarks, which explains their very small values, see Ref. [2] for a recent review. Interest in measurements of A_{PV} in nucleon-nucleon (NN) or in light nuclear systems at low incoming neutron energies is therefore motivated by the effort to find additional insight to the structure of the HWI, the least-known part of the weak interaction [3–7]. As shown below, the A_{PC} is directly sensitive to the strong and electromagnetic components of the nuclear interaction, and contributions from the HWI can be safely neglected since they are estimated to be a few orders of magnitude smaller. Because A_{PC} is a consequence of the interference between S and P waves of the incoming neutron at meV energies, $A_{PC} \propto 1/\lambda$, where λ is the neutron wavelength. More specifically, the scale of the A_{PC} will be proportional to (kR), where $k = 2\pi/\lambda$ and R a characteristic length for this reaction. For $\lambda = 5 \times 10^5$ fm, the neutron wave vector is $k \approx 1.3 \times 10^{-5}$ fm^{-1} and using $R \approx 1.97$ fm for the ^{3}He radius, we find the scale of A_{PC} to be $(kR) \approx 10^{-5}$.

For the unpolarized ^{3}He$(n, p)^3$H reaction, measurements of the total cross section and the differential cross section exist at very low energies. No data for PC polarization observables were reported for this reaction, only for the mirror reaction ^{3}H$(\vec{p}, \vec{n})^3$He [8,9]. These experiments were performed at proton incident energies corresponding to neutron energies of 300 keV or greater. Therefore, the measurement that we discuss here is the first ever measurement of a PC ^{3}He$(\vec{n}, p)^3$H polarization observable at meV incident neutron energies.

Since the four-nucleon scattering problem can be routinely solved, A_{PC} can be accurately calculated starting from a given model of the strong and electromagnetic interactions [10–17]. This observable is usually very sensitive to the nuclear interaction, in particular, to spin-orbit components of the NN interaction and the three-nucleon (3N) force. This can be readily understood, since A_{PC} is a consequence of the interaction in P waves. It is worth mentioning that in the physics of few-nucleon systems, we still have various discrepancies between theory and experiment, such as the famous analyzing power "A_y puzzle" in p-d, n-d, and p-^{3}He scattering [10,18–22]. In the present case, this sensitivity could be amplified since the process under study is at an energy rather close to the energy of the second excited state of ^{4}He, that has quantum numbers $J^\pi = 0^-$ [23]. Therefore, the study of this PC observable could be an extraordinary opportunity to study this poorly known resonance.

The energy spectrum of ^{4}He is, in fact, an important testing ground for understanding nuclear dynamics. Energies and widths of the various resonances have been determined in R-matrix analyses [23]. As a matter of fact, all excited states are resonances; however, their precise energies and widths contain critical information. Their calculation using different Hamiltonians gives slightly different results [9]. The first excited state, a 0^+ resonance, has been vigorously investigated both theoretically and experimentally. Without the Coulomb interaction, it would be a true bound state, with an energy well in agreement with that predicted in the framework of $A = 4$ Efimov physics [24]. This state has been studied experimentally by means of electron scattering, see Ref. [25] for a recent analysis. Theoretical studies have found that the position and width of this resonance are critically dependent on the interaction [26–30]. The next excited state, the 0^- resonance, is just above the threshold of n-^{3}He dissociation, and has a similar width as the 0^+ resonance. Its existence is due to the interaction in P waves.

Measurement and analysis of A_{PC}. In the ^{3}He$(\vec{n}, p)^3$H reaction the A_{PV} and the A_{PC} are orthogonal asymmetries that in a measurement are mixed by the experimental inaccuracies. In order to determine the mixing correction δA_{PC} on the A_{PV}, the A_{PC} has to be determined at the same neutron energy range as the A_{PV} was, see Ref. [1]. During the data runs of these two measurements the systematic uncertainties were controlled by performing the two asymmetry measurements so that the only change between the A_{PV} and A_{PC} setups was a rotation of the target/detector chamber around the beam axis to the most sensitive detector orientation and in addition, the two asymmetries were measured by alternating beam time between the two orientations [1]. The A_{PC} data and its quality is discussed in Ref. [1]. The asymmetries were calculated integrating detector yields over a neutron wavelength range of 3.4–6.3 Å, which was possible for the PV asymmetry, since it does not depend on incident neutron wavelength as the PC asymmetry does. Using the least-squares fit of the measured signal wire pair asymmetries from the A_{PV} and from the A_{PC} data sets, the uncorrected values for the A_{PV} and the A_{PC} were obtained. The fit resulted in the published uncorrected $A_{PC}^{unc} = [-41 \pm 5.6(\text{stat})] \times 10^{-8}$ [1]. The $1/\lambda$ dependence of A_{PC} is taken into account in the analysis of the A_{PC} datum in this Letter.

Corrections and systematic uncertainties for A_{PC}^{unc} are mainly due to the uncertainty in the detector chamber orientation. The first two corrections are due to a twist of the signal wire plane in the detector [1] and then the alignment uncertainty of the detector with the spin holding magnetic field. These two alignment uncertainties mix the small PV value into the significantly larger PC value, and are therefore expected to be small. The calculated plane twist and the field alignment corrections to A_{PC}^{unc} are -0.09 ± 0.00 ppb and 0.00 ± 0.04 ppb, respectively [1].

The origin of the third additive correction is the spin-orbit component of the electromagnetic neutron-^{3}He atom interaction due to the Mott-Schwinger (MS) mechanism [31]. In fact, the probability that a neutron undergoes an elastic scattering on ^{3}He atoms in the target before being captured by another helium nucleus is very small, $\approx 10^{-4}$, but, in any case, finite. This elastic scattering produces, via the MS mechanism, a small left-right asymmetry A_{MS} that is then conserved in the subsequent capture, which is essentially isotropic. The sequence (elastic scattering + capture) produces at the end a false asymmetry δA_{MS}, which has to be subtracted from A_{PC}^{unc}

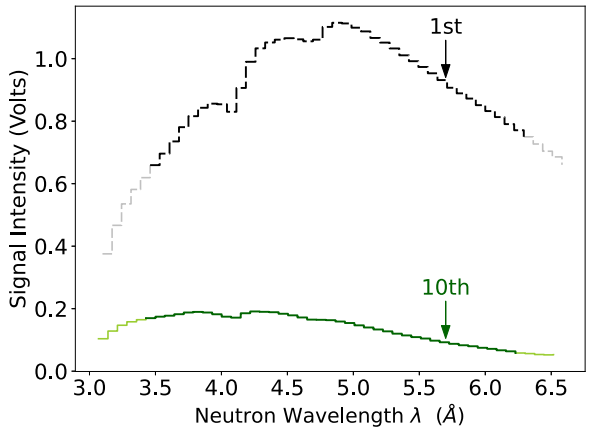

FIG. 1. The selected measured outputs of the central signal wires of the first and the tenth wire planes out of 16 planes. The plots indicate how the incoming beam intensity and shape change as it passes through the ^{3}He gas in the chamber. The signals were measured as a function of TOF but are plotted as a function of the neutron wavelength. Due to 17 cm difference in distance between the two wire planes from the moderator, the neutron wavelengths on the tenth are little shorter than on the first wire, consequently, there is a half time bin shift between the wavelength plots. The signals represent collected charges after the emitted proton and triton from the n^3He capture deposit their kinetic energy to ^{3}He gas, see text for details. The integration ranges of the two signals are indicated with thicker lines. The two small dips at 4.1 Å and 4.7 Å are residuals from neutron transmission Bragg-edges on the aluminum beam-line windows.

in order to obtain the PC asymmetry due solely to the capture process. We calculated $A_{\rm MS}$ following the model described in Ref. [31]. Since it depends on the neutron wavelength λ, we have to average over the measured wavelength range at each wire plane j (the geometry of the detector chamber is discussed in the Supplemental Material [32]).

$$\bar{A}^{\rm j}_{\rm MS} = \int_{\lambda^{\rm j}_{\rm min}}^{\lambda^{\rm j}_{\rm max}} A^{\rm j}_{\rm MS}(\lambda) P^{\rm j}(\lambda) {\rm d}\lambda, \tag{2}$$

where $P^{\rm j}(\lambda)$ is the yield density distribution of the wire plane. Figure 1 shows yields from two out of 16 central signal wires of the first and the tenth plane. $\lambda^{\rm j}_{\rm min(max)}$ are the integration limits, unique in each wire plane due to the increasing distance of the planes from the moderator. The significant variation in the detector yield between the planes is due mainly to the large wavelength-dependent n-^{3}He capture cross section [33,34] that exponentially decreases the beam intensity as it passes through the ^{3}He gas at a pressure of 43.6 kPa. The overall MS asymmetry $\bar{A}_{\rm MS}$ for the detector is obtained by calculating the average given in Eq. (2) for each of the 16 wire planes and then combining those using the integrated yield in the respective planes as the weighting factor. The final calculated value is $\bar{A}_{\rm MS} = (-4.8 \pm 0.2) \times 10^{-5}$. This number, multiplied by the fraction of neutrons that first undergo elastic scattering instead of capture (estimated by the ratio of the corresponding phenomenological cross sections [34,35], see the Supplemental Material [32]), gives the correction to $A_{\rm PC}$, which turns out to be $\overline{\delta A}_{\rm MS} = (-1.32 \pm 0.10) \times 10^{-8}$. With the above corrections and those from Table 1 of Ref. [1], we obtain the final value for the measured PC asymmetry

$$A_{\rm PC} = [-42.5 \pm 6.0({\rm stat}) \pm 0.11({\rm sys})] \times 10^{-8}, \tag{3}$$

where the error in the calculated value of $\overline{\delta A}_{\rm MS}$ has been folded into the systematic uncertainty.

The incoming neutrons contributing to the PC asymmetry reported in Eq. (3) have a range of wavelengths. Since $A_{\rm PC} \propto 1/\lambda$, we can write explicitly

$$A_{\rm PC}(\mu) = \beta\mu, \tag{4}$$

where β is a constant that we want to extract from $A_{\rm PC}$ and $\mu \equiv 1/\lambda$. The mean inverse wavelength over the integrated wave forms in each wire plane can be calculated as discussed previously in context of Eq. (2) and in Supplemental Material [32]. For the overall $\overline{\mu}$ we obtain

$$\overline{\mu} \equiv \left\langle \frac{1}{\lambda} \right\rangle = 0.2151 \pm 0.0015 \ {\rm Å}^{-1}, \tag{5}$$

where the uncertainty is statistical, and is determined by the averaging process.

To finalize systematic uncertainties in β, we need to work out first the full uncertainties in $\overline{\mu}$. The wavelength of neutrons arriving at detector location is calculated from the measured time of flight (TOF) over the known neutron path length. In our case, the path length is formed by a distance from the neutron emission surface from the liquid hydrogen moderator to the first wire plane in the detector, this distance has been measured with relative accuracy of 0.2%. The TOF measurement is started by a clock signal corresponding to the arrival of the proton beam bunch on the mercury target to within 1 μs, a small correction to TOF is coming from the neutron emission time, i.e., the time from start of TOF to moment when the neutron exits the moderator [36]. After a selected delay (13.500 ms), the DAQ system starts to digitize the signals in 49 time bins of 0.32 ms width. Figure 1 shows typical detector yields, measured in the first and tenth wire planes as a function of TOF but presented as a function of wavelength. This presentation required that the two plots had to be shifted a little respect to the x axis, since the two planes are at different distances from the moderator. The TOF calculation includes as its most significant uncertainty the charge collection time, the time that is required to collect all the charges from the ionization by the emitted proton from the n-^{3}He capture. Results of GARFIELD++ simulations indicate that the collection time can be up to 1.5 ms long [37]. This is the dominating uncertainty in $\overline{\mu}$ and is carried over to the systematic uncertainty in β. A more detailed discussion of the determination of the uncertainty is contained in the Supplemental Material [32]. Our final result for β is

$$\beta = [-1.97 \pm 0.28\,({\rm stat}) \pm 0.12\,({\rm sys})] \times 10^{-6}\ {\rm Å}. \tag{6}$$

Note that without this systematic error in μ, the systematic error in β would be reduced to 0.02×10^{-6} Å.

Theoretical analysis. In the Letter the four-nucleon (4N) scattering problem is solved using the hyperspherical harmonics (HH) method [9,38]. Here, we will give only some details

of the procedure. First, a particular clusterization $A+B$ of the four-nucleon system in the asymptotic region is denoted with the index γ. More specifically, $\gamma=1$ (2) corresponds to p-^{3}H (n-^{3}He) clusterization. Consider a scattering state with total angular momentum quantum number JJ_z, and parity π. The asymptotic part of the wave function describing the incoming clusters γ with relative orbital angular momentum L and total spin S [note that $\pi\equiv(-)^L$] is generally written as a sum of a (distorted) plane wave plus outgoing spherical waves in all possible channels γ', L', S'. The weights of the outgoing waves are the T-matrix elements (TMEs) ${}^J T^{\gamma,\gamma'}_{LS,L'S'}$. It is well known that ${}^J T^{2,1}_{LS,L'S'} \approx q_2^L$ for $q_2\to 0$ (see Sec. IV of Ref. [39]), where q_2 is the relative n-^{3}He momentum. To complete the calculation, the inner part of the wave function (where the nucleons are close between themselves) is described by an expansion over the HH basis (for more details, see Refs. [9,39]).

In terms of the TMEs, the transverse asymmetry can be written as

$$\begin{aligned} A_{\rm PC}\sigma_0 = {}& 3\sqrt{2}\Im\left[\left({}^1T^{2,1}_{11,10}\right)^*\,{}^0T^{2,1}_{00,00}\right] + 2\Im\left[\left({}^0T^{2,1}_{11,11}\right)^*\,{}^1T^{2,1}_{01,01}\right] \\ & + 3\sqrt{2}\Im\left[\left({}^1T^{2,1}_{10,11}\right)^*\,{}^1T^{2,1}_{01,01}\right] \\ & + 3\sqrt{2}\Im\left[\left({}^1T^{2,1}_{11,11}\right)^*\,{}^1T^{2,1}_{01,01}\right] \\ & - 5\Im\left[\left({}^2T^{2,1}_{11,11}\right)^*\,{}^1T^{2,1}_{01,01}\right], \end{aligned} \tag{7}$$

$$\sigma_0 = \left|{}^0T^{2,1}_{00,00}\right|^2 + 3\left|{}^1T^{2,1}_{01,01}\right|^2, \tag{8}$$

where in the expression of σ_0 we have retained only the contributions of S-wave TMEs (which are $\approx q_2^0$), and in $A_{\rm PC}$ the contribution of S and P waves. From the q_2 behavior discussed above, we see that $A_{\rm PC}\approx q_2$. Note that $q_2=(3/4)2\pi/\lambda$, hence $A_{\rm PC}\approx 1/\lambda$ as discussed previously.

The $A_{\rm PC}$ observable has been obtained using the NN interaction derived by Entem and Machleidt at next-to-next-to-next-leading order (N3LO) in chiral effective field theory (EFT) [40,41], corresponding to two different cutoff values ($\Lambda=500$ MeV and $\Lambda=600$ MeV). These NN interactions are labeled, respectively, N3LO500 and N3LO600. The parameter Λ is used to cut the interaction for momentum transfer $k\gtrsim\Lambda$, or equivalently at interparticle distances $r\lesssim 1/\Lambda$. They reflect our ignorance of the short-range physics, which is taken into account by a number of low-energy constants entering the expression of the potential, and fitted to the NN database. Roughly, at the end of the procedure, the calculated observables should be independent of Λ. The eventual dependence on Λ of the results indicates that the order of the potential (N3LO in this case) is not sufficient to describe the observable under study. This rationale should be refined and made consistent by studying the observable with interaction derived at various orders, and using a Bayesian analysis to study the theoretical uncertainty associated to the truncation of the chiral expansion [42–45]. Clearly this analysis (in progress) should be performed by including 3N forces derived at the same order as the NN interaction.

The 3N force considered here has been derived at next-to-next-leading order (N2LO) in Ref. [46] (the 3N force contributions at N3LO and beyond are still under construction but we plan to include them in future 4N calculations). With the N3LO500 (N3LO600) NN interaction, we have considered the 3N N2LO force, in the local coordinate space version [47], labeled N2LO500 (N2LO600). These interactions include the contribution of a two-pion-exchange, an one-pion-exchange, and a 3N contact interaction diagram as derived in chiral PT [46]. The contribution of the last two diagrams involves two new LECs, known as the parameters c_D and c_E, respectively. They have been fixed by reproducing two observables in the 3N systems, i.e., the 3N binding energy and the experimental Gamow-Teller (GT) matrix element in the tritium beta decay [48–50]. The values of these parameters, recently redetermined in Ref. [50], are $(c_D, c_E) = (+0.945, -0.0410)$ for the N2LO500 force and $(c_D, c_E) = (+1.145, -0.6095)$ for the N2LO600 force. For example, in the following a calculation performed with the N3LO500 NN interaction plus N2LO500 3N interaction will be denoted as N3LO500+N2LO500, etc.

In order to explore the dependence on the parameters c_D and c_E, we use also another 3N N2LO force labeled N2LO500*. In this case, the interaction reproduces the 3N binding energies but not the tritium GT matrix element. The corresponding values of the parameters are chosen arbitrarily to be $(c_D, c_E) = (-0.12, -0.196)$. The calculation based on this interaction will be labeled N3LO500+N2LO500*.

We also report results obtained using the Norfolk NN interactions, also derived within chiral EFT, but using as degrees of freedom nucleons, pions and Δs [51,52]. In this case, the potentials are regularized in coordinate space. We use the so-called NVIa and NVIb NN interactions, regularized with cutoff $R_L=1.2$ and 1.0 fm, respectively. They are augmented by 3N N2LO interactions, with $(c_D, c_E) = (-0.635, -0.090)$ for the NVIa force and $(c_D, c_E) = (-4.71, +0.55)$ for the NVIb force (see Table IV of Ref. [53]). The calculations based on these interactions will be labeled NVIa+N2LOa and NVIb+N2LOb, respectively.

In all cases, the electromagnetic force between the nucleons has been approximated by the point-Coulomb potential. Effects due to other terms, as the magnetic dipole interaction, the vacuum polarization term, etc. are thought to be very small in capture observables.

For each interaction, the convergence of the calculated TMEs has been checked by increasing the size of the HH basis. The only problematic quantity to be calculated has been found to be the 0^- TME, due to the difficulty of constructing the 4N wave function close to the 0^- resonance.

In order to explore the properties of this resonance, we have performed a series of calculations for different neutron energies. From the TMEs we can extract also the resonance position $E_{\rm R}$ and width Γ, using the procedure described in Ref. [9], Sec. IV B. Results are reported in columns 2 and 3 of Table I. The values are generally smaller than those extracted from the experiment using an R-matrix analysis [23] (actually, the two methods do not necessarily give the same result). The $E_{\rm R}$ value in correspondence with the N3LO500+N2LO500 interaction is found to be smaller than for the other cases. Also the width Γ is found to be narrower. We note that $A_{\rm PC}$ is very sensitive to the value of ${}^0t^{2,1}_{11,11} = \lim_{q_2\to 0}|{}^0T^{2,1}_{11,11}|/q_2$,

TABLE I. Results of the calculations performed using the HH method. The calculations reported in the first part of the table have been performed considering Hamiltonians with only a NN interaction, while in the second part also a 3N potential has been included. See the main text for the notation adopted. In columns 2 and 3, we report the position E_R and width Γ of the ^{4}He 0^- resonance obtained as discussed in Ref. [9]. Note that E_R is calculated starting from the n-^{3}He threshold. In column 4, we report the values of ${}^0t^{2,1}_{11,11} = \lim_{q_2\to 0} |{}^0T^{2,1}_{11,11}|/q_2$ and in column 5 the quantity β as defined in Eq. (4) (we remind that this quantity at low energies is independent of q_2). In the last row, we report the experimental values for E_R, Γ [23], and β, the latter quantity obtained as discussed in the main text.

Interaction	E_R (MeV)	Γ (MeV)	${}^0t^{2,1}_{11,11}$ (fm)	$\beta \times 10^6$ (Å)
N3LO500	0.16	0.41	20.7	−4.83
N3LO600	0.24	0.51	16.9	−2.68
NVIa	0.31	0.53	17.3	−2.61
NVIb	0.30	0.54	13.0	−0.43
N3LO500+N2LO500	0.06	0.26	30.1	−10.04
N3LO500+N2LO500*	0.14	0.41	18.5	−2.68
N3LO600+N2LO600	0.09	0.30	25.9	−5.28
NVIa+N2LOa	0.04	0.36	35.4	−12.17
NVIb+N2LOb	0.12	0.40	23.9	−5.15
Experimental	0.44	0.84		−1.97 ±0.28 (stat) ±0.12 (sys)

reported in the fourth column of the table. Note the large variation with the different interactions. Tiny differences of the position of the 0^- resonance result in large changes in ${}^0t^{2,1}_{11,11}$.

Finally, in column 5 we report the calculated values of $\beta = A_{PC} \times \lambda$ for the various interactions using Eq. (7). The calculations have been performed at $q_2 = 0$ (namely, at $\lambda \to \infty$), but in any case, for these energies β is independent of q_2. The large differences between the results for β reflect the fact that the various terms in Eq. (7) tend to cancel each other, in particular the first two, which are the largest ones. Furthermore, note that without the contribution of the ${}^0T^{2,1}_{11,11}$ term, A_{PC} would be positive, at variance with what is found experimentally. The A_{PC} with N3LO500+N2LO500 is found to be too large (in absolute value), due to the large value of ${}^0T^{2,1}_{11,11}/q_2$. This is probably a consequence of the fact that for this interaction the 0^- resonance is very close to the n-^{3}He threshold.

The interaction N3LO500+N2LO500* differs from N3LO500+N2LO500 just for c_D, c_E values. In this case A_{PC} is found to be in good agreement with the experimental value. This result shows the sensitivity of this observable to the details of the 3N force. The difference between the N3LO500+N2LO500 and N3LO600+N2LO600 results shows the sensitivity of this observable to the cutoff values and consequently to the different treatment of the short-range physics.

Conclusions. The first accurate measurement of a parity-conserving proton directional asymmetry at reaction of ^{3}He($\vec{n}$, p)^{3}H at meV incident neutron energies resulted in $A_{PC} = [-42.5 \pm 6.0(\text{stat}) \pm 0.11(\text{sys})] \times 10^{-8}$. Since the A_{PC} depends on $1/\lambda$, where λ is neutron wavelength, we can remove the λ dependence and obtain a constant $\beta = (\lambda \times A_{PC}) = [-1.97 \pm 0.28\,(\text{stat}) \pm 0.12\,(\text{sys})] \times 10^{-6}$ Å. In this reaction, A_{PC} comes out from the S- and P-wave interference induced mainly by the strong nuclear interaction. The difference between the final A_{PC} and the uncorrected A^{unc}_{PC} [1] is only 3%; this small improvement in the A_{PC} does not cause any significant corrections to the published $A_{PV} = [1.55 \pm 0.97\,(\text{stat}) \pm 0.24\,(\text{sys})] \times 10^{-8}$ [1].

This accurate measurement of the A_{PC} represents an important testing ground for nuclear physics studies, in particular those involving polarized neutrons. We have calculated A_{PC} using a number of modern nuclear interactions derived in the framework of chiral EFT. We have found that this observable depends critically on the 0^- TME. This quantity is in turn very sensitive to the nuclear Hamiltonian, since the experiment is performed at an energy close to a rather sharp 0^- resonance in the ^{4}He spectrum. Thus, this observable works like a magnifying glass for the nuclear dynamics, and in particular for NN P-wave and 3N interactions, so that this study can give valuable information on these small components of the interaction and can be very useful in order to construct more accurate nuclear potentials. This can have a noticeable impact on other studies where the accurate determination of the nuclear matrix elements is crucial, as, for instance, in the case of the neutrinoless double beta decay.

To summarize, this Letter reports a preliminary study of this observable using a number of interactions, in order to show its extreme sensitivity to the NN and 3N interactions. In particular, this observable could be used to fix the 3N interaction in P waves. This could be accomplished by using the 3N interaction at N4LO, where a certain number of new and unknown LECs appear [54,55]. At present the effect of these components are being constrained in the 3N system. Their effects in $A = 4$ systems (and for this observable) will be performed after this preliminary part is concluded.

Finally, we comment on the impact of this study on the PV observable A_{PV}. As we have seen, the difficulty in the prediction of A_{PC} is due to the large variability in the TME ${}^0T^{2,1}_{11,11}$. However, this element does not enter in the calculation of A_{PV} (it is suppressed with respect to other terms by a factor $\approx q_2$). Therefore, the theoretical prediction of A_{PV} is much less sensitive to the choice of the strong Hamiltonian.

Acknowledgments. We gratefully acknowledge the support of the U.S. Department of Energy Office of Nuclear Physics through Grants No. DE-FG02-03ER41258, No. DE-AC05-00OR22725, No. DE-SC0008107, and No. DE-SC0014622, the US National Science Foundation Award No: PHY-0855584, the Natural Sciences and Engineering Research Council of Canada (NSERC), the Canadian Foundation for Innovation (CFI), and the Mexican PAPIIT-UNAM Awards No. IN111913 and No. AG102023. The measurements were conducted with the Fundamental Neutron Physics Beamline (FNPB) 13B at the Spallation Neutron Source (SNS), a Department of Energy (DOE) Office of Science (SC) User Facility operated by Oak Ridge National Laboratory (ORNL).

[1] M. T. Gericke *et al.* (The n3He Collaboration), Phys. Rev. Lett. **125**, 131803 (2020).
[2] J. de Vries, E. Epelbaum, L. Girlanda, A. Gnech, E. Mereghetti, and M. Viviani, Front. Phys. **8**, 218 (2020).
[3] M. J. Ramsey-Musolf and S. A. Page, Annu. Rev. Nucl. Part. Sci. **56**, 1 (2006).
[4] W. C. Haxton and B. R. Holstein, Prog. Part. Nucl. Phys. **71**, 185 (2013).
[5] M. R. Schindler and R. P. Springer, Prog. Part. Nucl. Phys. **72**, 1 (2013).
[6] B. Desplanques, J. F. Donoghue, and B. R. Holstein, Ann. Phys. (NY) **124**, 449 (1980).
[7] D. B. Kaplan and M. J. Savage, Nucl. Phys. A **556**, 653 (1993); **570**, 833(E) (1994); **580**, 679(E) (1994).
[8] See, for example, https://www-nds.iaea.org/exfor/.
[9] M. Viviani, L. Girlanda, A. Kievsky, and L. E. Marcucci, Phys. Rev. C **102**, 034007 (2020).
[10] A. Deltuva and A. C. Fonseca, Phys. Rev. C **75**, 014005 (2007); Phys. Rev. Lett. **98**, 162502 (2007); Phys. Rev. C **76**, 021001(R) (2007).
[11] A. Deltuva and A. C. Fonseca, Phys. Rev. C **95**, 024003 (2017).
[12] R. Lazauskas, Phys. Rev. C **79**, 054007 (2009).
[13] R. Lazauskas and J. Carbonell, Front. Phys. **7**, 251 (2020).
[14] B. Pfitzinger, H. M. Hofmann, and G. M. Hale, Phys. Rev. C **64**, 044003 (2001).
[15] P. Navratil, R. Roth, and S. Quaglioni, Phys. Rev. C **82**, 034609 (2010).
[16] S. Aoyama, K. Arai, Y. Suzuki, P. Descouvemont, and D. Baye, Few-Body Syst. **52**, 97 (2012).
[17] M. Viviani, A. Deltuva, R. Lazauskas, A. C. Fonseca, A. Kievsky, and L. E. Marcucci, Phys. Rev. C **95**, 034003 (2017).
[18] Y. Koike and J. Haidenbauer, Nucl. Phys. A **463**, 365 (1987).
[19] H. Witala, W. Glöckle, and T. Cornelius, Nucl. Phys. A **491**, 157 (1989).
[20] A. Kievsky *et al.*, Nucl. Phys. A **607**, 402 (1996).
[21] A. C. Fonseca, Phys. Rev. Lett. **83**, 4021 (1999).
[22] M. Viviani, L. Girlanda, A. Kievsky, and L. E. Marcucci, Phys. Rev. Lett. **111**, 172302 (2013).
[23] D. R. Tilley, H. R. Weller, and G. M. Hale, Nucl. Phys. A **541**, 1 (1992).
[24] A. Kievsky, L. Girlanda, M. Gattobigio, and M. Viviani, Annu. Rev. Nucl. Part. Sci. **71**, 465 (2021).
[25] S. Kegel *et al.*, Phys. Rev. Lett. **130**, 152502 (2023).
[26] E. Hiyama, B. F. Gibson, and M. Kamimura, Phys. Rev. C **70**, 031001(R) (2004).
[27] S. Bacca, N. Barnea, W. Leidemann, and G. Orlandini, Phys. Rev. Lett. **110**, 042503 (2013).
[28] S. Bacca, N. Barnea, W. Leidemann, and G. Orlandini, Phys. Rev. C **91**, 024303 (2015).
[29] N. Michel, W. Nazarewicz, and M. Ploszajczak, Phys. Rev. Lett. **131**, 242502 (2023).
[30] Ulf-G. Meißner, S. Shen, S. Elhatisari, and D. Lee, Phys. Rev. Lett. **132**, 066604 (2024).
[31] M. T. Gericke, J. D. Bowman, and M. B. Johnson, Phys. Rev. C **78**, 044003 (2008).
[32] See Supplemental Material at http://link.aps.org/supplemental/10.1103/PhysRevC.110.L061001 for a detailed discussion of the determination of the systematic uncertainty of the parameter β.
[33] Neutron scattering lengths and cross sections, Neutron News **3**, 29 (1992).
[34] J. Als-Nielsen and O. Dietrich, Phys. Rev. **133**, B925 (1964).
[35] V. P. Alfimenkov, S. B. Borzakov, Y. Vezhbitski, A. M. Govorov, L. B. Pikelner, and E. I. Sharapov, Rept: Joint Inst. for Nucl. Res., Dubna Reports 80–394, 1980.
[36] W. Lu, SNS-106100200-TR0199-R00, 2013.
[37] M. McCrea, Parity Violation and Cold Neutron Capture: A study of the detailed interaction between hadrons, Ph.D. thesis, University of Manitoba, Winnipeg (Canada), 2016.
[38] L. E. Marcucci, J. Dohet-Eraly, L. Girlanda, A. Gnech, A. Kievsky, and M. Viviani, Front. Phys. **8**, 69 (2020).
[39] M. Viviani, R. Schiavilla, L. Girlanda, A. Kievsky, and L. E. Marcucci, Phys. Rev. C **82**, 044001 (2010).
[40] D. R. Entem and R. Machleidt, Phys. Rev. C **68**, 041001(R) (2003).
[41] R. Machleidt and D. R. Entem, Phys. Rep. **503**, 1 (2011).
[42] R. J. Furnstahl, N. Klco, D. R. Phillips, and S. Wesolowski, Phys. Rev. C **92**, 024005 (2015).
[43] S. Wesolowski, N. Klco, R. J. Furnstahl, D. R. Phillips, and A. Thapaliya, J. Phys. G: Nucl. Part. Phys. **43**, 074001 (2016).
[44] S. Wesolowski *et al.*, Phys. Rev. C **104**, 064001 (2021).
[45] A. Gnech, L. E. Marcucci, and M. Viviani, Phys. Rev. C **109**, 035502 (2024).
[46] E. Epelbaum, A. Nogga, W. Glockle, H. Kamada, Ulf-G. Meissner, and H. Witala, Phys. Rev. C **66**, 064001 (2002).
[47] P. Navrátil, Few-Body Syst. **41**, 117 (2007).
[48] A. Gardestig and D. R. Phillips, Phys. Rev. Lett. **96**, 232301 (2006).
[49] D. Gazit, S. Quaglioni, and P. Navrátil, Phys. Rev. Lett. **103**, 102502 (2009).
[50] L. E. Marcucci, A. Kievsky, S. Rosati, R. Schiavilla, and M. Viviani, Phys. Rev. Lett. **121**, 049901(E) (2018).
[51] M. Piarulli, L. Girlanda, R. Schiavilla, A. Kievsky, A. Lovato, L. E. Marcucci, S. C. Pieper, M. Viviani, and R. B. Wiringa, Phys. Rev. C **94**, 054007 (2016).
[52] M. Piarulli, A. Baroni, L. Girlanda, A. Kievsky, A. Lovato, E. Lusk, L. E. Marcucci, S. C. Pieper, R. Schiavilla, M. Viviani, and R. B. Wiringa, Phys. Rev. Lett. **120**, 052503 (2018).
[53] A. Baroni *et al.*, Phys. Rev. C **98**, 044003 (2018).
[54] L. Girlanda, A. Kievsky, L. E. Marcucci, and M. Viviani, Phys. Rev. C **102**, 064003 (2020).
[55] L. Girlanda, E. Filandri, A. Kievsky, L. E. Marcucci, and M. Viviani, Phys. Rev. C **107**, L061001 (2023).